Received: 29 August 2016 | Revised: 17 February 2017 | Accepted: 27 February 2017

DOI: 10.1002/nbm.3726

WILEY NMR IN BIOMEDICINE

RESEARCH ARTICLE

^{17}O MRS assesses the effect of mild hypothermia on oxygen consumption rate in tumors

Marie-Aline Neveu[1] | Nicolas Joudiou[1] | Géraldine De Preter[1] | Jean-Paul Dehoux[2] | Bénédicte F. Jordan[1] | Bernard Gallez[1]

[1] Biomedical Magnetic Resonance Research Group, Louvain Drug Research Institute (LDRI), Université catholique de Louvain (UCL), Belgium

[2] Experimental Surgery Unit, Medical School, Institute of Experimental and Clinical Research (IREC), Université catholique de Louvain (UCL), Belgium

Correspondence
B. Gallez, Biomedical Magnetic Resonance Unit – REMA, Louvain Drug Research Institute (LDRI), Université catholique de Louvain, Avenue Mounier, 73.08, B-1200 Brussels, Belgium.
Email: bernard.gallez@uclouvain.be

Funding Information
Belgian National Fund for Scientific Research (FNRS), Grant/Award Number: PDR T.0107.13; Télévie, Grant/Award Number: 7.4578.13; Action de Recherches Concertées, Grant/Award Number: 14/19-058

Although oxygen consumption is a key factor in metabolic phenotyping, its assessment in tumors remains critical, as current technologies generally display poor specificity. The objectives of this study were to explore the feasibility of direct ^{17}O nuclear magnetic resonance (NMR) spectroscopy to assess oxygen metabolism in tumors and its modulations. To investigate the impact of hypometabolism induction in the murine fibrosarcoma FSAII tumor model, we monitored the oxygen consumption of normothermic (37°C) and hypothermic (32°C) tumor-bearing mice. Hypothermic animals showed an increase in tumor pO_2 (measured by electron paramagnetic resonance oximetry) contrary to normothermic animals. This was related to a decrease in oxygen consumption rate (assessed using ^{17}O magnetic resonance spectroscopy (MRS) after the inhalation of $^{17}O_2$-enriched gas). This study highlights the ability of direct ^{17}O MRS to measure oxygen metabolism in tumors and modulations of tumor oxygen consumption rate.

KEYWORDS

direct ^{17}O MRS, EPR, oxygen consumption, tumor hypoxia

1 | INTRODUCTION

Although ^{17}O nuclear magnetic resonance (NMR) spectroscopy has been utilized for a long time in the life sciences,[1-3] modern instrumentation has allowed the development of both ^{17}O magnetic resonance spectroscopy (MRS) and ^{17}O magnetic resonance imaging (MRI).[4-8] During oxidative metabolism, molecular oxygen is converted into water at a rate dependent on the metabolic activity in tissues. This conversion can be monitored using ^{17}O MRS. During the inhalation of ^{17}O–enriched oxygen gas ($^{17}O_2$), the metabolic inclusion of the ^{17}O atom in water molecules and the appearance of the water peak ($H_2{}^{17}O$) reflect the local oxygen consumption. As a result of specific detection of $H_2{}^{17}O$ using direct ^{17}O MRS *in vivo*, this non-invasive technique allows the measurement and quantification of subtle dynamic changes in metabolic $H_2{}^{17}O$ and oxygen consumption rate.[9-16]

Oxygen plays a key role in cellular metabolism. As a major oxidizer, O_2 is involved in the catabolism of fuel molecules and energy production. O_2 metabolism is thus highly regulated to adjust to the metabolic requirements and to ensure normal tissue function. Direct ^{17}O NMR *in vivo* has been used to study O_2 metabolism in the brain[9-16] and heart.[17,18] These organs strongly rely on oxygen to produce energy, and many brain and heart diseases have been linked to abnormal O_2 metabolism. Recently, the tumor oxygen consumption rate has also been appraised using this technique.[19,20] For a long time, tumor cells have been considered to be defective in mitochondrial oxygen consumption because of their dominant glycolytic metabolism.[21,22] However, new evidence on the oxidative activities in tumor cells has challenged this paradigm.[23-26] Metabolic characterization *in vivo* could change the understanding of tumor metabolism and could allow the identification of new targets for innovative anti-cancer strategies.

Marie-Aline Neveu and Nicolas Joudiou contributed equally to this work.

Abbreviations used: 3D FLASH, three-dimensional fast low-angle shot; BOLD, blood oxygenation level-dependent; BW, bandwidth; $CMRO_2$, cerebral metabolic rate of oxygen; EPR, electron paramagnetic resonance; FA, flip angle; FID, free induction decay; FOV, field of view; $H_2{}^{17}O$, ^{17}O–labeled water; MRS, magnetic resonance spectroscopy; NA, number of averages; NMR, nuclear magnetic resonance; $^{17}O_2$, ^{17}O–enriched oxygen gas; PET, positron emission tomography; RARE, rapid acquisition with relaxation enhancement; RF, radiofrequency; ROI, region of interest; SEM, standard error of the mean; SNR, signal-to-noise ratio

 Copyright © 2017 John Wiley & Sons, Ltd.

The objectives of this study were to explore the feasibility of direct ^{17}O MRS to assess oxygen metabolism in tumors and its modulations. To investigate the impact of hypometabolism induction in the murine fibrosarcoma FSAII tumor model, we monitored the oxygen consumption of normothermic (37°C) and hypothermic (32°C) tumor-bearing mice. We first evaluated the effect of mild hypothermia on tumor oxygenation. Using electron paramagnetic resonance (EPR), we observed an increase in pO_2 in hypothermic FSAII tumors which was not observed under normothermic conditions. We then studied oxygen consumption in FSAII tumors using a direct ^{17}O MRS approach. We showed that the induction of mild hypothermia had a profound effect on tumor oxygen consumption in the tumor model. This study highlights the ability of direct ^{17}O MRS to quantitatively assess oxygen metabolism in tumors.

2 | EXPERIMENTAL DETAILS

2.1 | Animal preparation

Animal studies were undertaken in accordance with Belgian and the Université catholique de Louvain ethical committee regulations (agreement numbers UCL/2010/MD/001 and UCL/2014/MD/026).

A total of 10^6 FSAII murine fibrosarcoma cells were inoculated subcutaneously into the hind thigh of C3H/HeOuJIco male mice (Janvier, Le Genest-Saint-Isle, France). Tumors were measured daily with an electronic caliper and the experiments were performed when tumors had reached 8 ± 1.0 mm in diameter (at this stage of tumor development, necrosis was characterized as limited[27,28]). During the experiments, animals were anesthetized by inhalation of isoflurane (Forene, Abbott, Queenborough, Kent, UK) mixed with air in a continuous flow (2 L/min), as this form of anesthesia has been shown to have a negligible effect on tissue hemodynamics.[29] Anesthesia was induced using 3% isoflurane; 1.5–2% isoflurane was then used to maintain respiration at a rate of 80 ± 10 breaths per minute during the experiments. A pressure cushion was used to monitor respiration during the experiments (SA Instruments Inc., Stony Brook, NY, USA). A circulating water system was used to regulate body temperature, and animal temperature was monitored using a rectal temperature probe (Bioseb, Vitrolles, France). For the normothermic condition, animal temperature was kept at 37 ± 0.5°C during the experiments. For the hypothermic condition, the water pump temperature was reduced to maintain the body temperature at 32 ± 0.5°C.

2.2 | EPR measurements

EPR oximetry was used as it provides quantitative and very sensitive measurements of tissue oxygenation. The method is also a relevant tool to calibrate other oxygen-sensitive methods, such as MRI and positron emission tomography (PET).[30-32]

In vivo tumor pO_2 was monitored by EPR spectroscopy using charcoal as the oxygen-sensitive probe.[33,34] EPR spectra were recorded using a 1.1-GHz EPR spectrometer (Magnettech, Berlin, Germany). According to calibration curves made by measuring the EPR line width as a function of pO_2,[35] the EPR spectral line width was converted to pO_2. A charcoal suspension (100 mg/mL) was injected intratumorally (60 µL), 24 h before the experiments. For EPR reading, the tumor under study was placed in the center of the extended loop resonator whose sensitive volume extends 1 cm into the tumor mass. The pO_2 measurements correspond to an average of pO_2 values in the tumor volume.

After the induction of mild hypothermia, pO_2 measurements were started when the body temperature of the mice reached 32°C. For the normothermic condition, measurements were performed after a 10-min equilibration period. For each condition, EPR spectra were recorded every 30 min during 2 h.

2.3 | Gas delivery system

The gas delivery system for $^{17}O_2$ inhalation experiments is presented in Figure 1. The animal was placed in a home-built closed system containing a nose cone, a circulating water system for body temperature regulation, a breathing monitoring system and space for the radiofrequency (RF) coil. The nose cone was attached to a breathing line connected to the main anesthesia line and to a $^{17}O_2$ delivery line controlled by a valve. Prefilled syringes were used to manually deliver the $^{17}O_2$ gas and ensure continuous delivery. $^{17}O_2$ gas (70% enriched, NUKEM Isotopes GmbH, Alzenau, Germany) and the isoflurane/N_2 gas mixture were stored in separate gas reservoirs (Tedlar® bag); 40 mL of $^{17}O_2$ gas were mixed with 160 mL of isoflurane (1.5%)/N_2 mixture. The final mixture was loaded into 100-mL syringes connected to the breathing line. To deliver the mixture, the breathing line was manually switched to the $^{17}O_2$ line. By applying pressure on the prefilled syringes, the $^{17}O_2$ mixture was delivered as a continuous flow during 2 min. Then, gas was switched back to the main anesthesia line. The valve and syringes connected to the $^{17}O_2$ line were placed as close to the outside of the magnet to limit the dead volume. Also, the home-built system holding the animal was closed during the experiments to limit gas dispersion.

2.4 | ^{17}O MRS measurements

For oxygen consumption experiments, direct ^{17}O MRS was performed on an 11.7-T instrument (Bruker Biospec) controlled by Paravision 6.0 (Bruker, Ettlingen, Germany). Experiments were carried out using a $^{1}H/^{17}O$ Bruker surface coil system (equivalent diameters of 2 cm) positioned over the tumor mass. Anatomical images were first acquired using a T_2-weighted axial turbo RARE (rapid acquisition with relaxation enhancement) sequence [TR = 2500 ms; TE = 30 ms; rare factor, 8; number of averages (NA) = 2; field of view (FOV), 25 × 25 mm^2; resolution, 98 × 98 μm^2; slice thickness, 1 mm]. ^{17}O MRS measurements were carried out using a non-localized, single-pulse sequence [TR = 16.5 ms; NA = 600; T_{acq} = 20 min (120 measurements); acquisition bandwidth (BW), 5000 Hz; flip angle (FA), 20°]. For the ^{17}O MRS sequence, the 90° reference pulse (0.405 ms) was optimized previously on natural abundance $H_2{}^{17}O$ samples.

To measure tumor oxygen consumption during $^{17}O_2$ delivery, a total of 120 ^{17}O spectra were collected in about 20 min, before, during and after a 2-min inhalation period of the $^{17}O_2$ mixture. No filter was applied on the free induction decay (FID). Phase correction was applied to the spectra. Then, the integrals of the $H_2{}^{17}O$ peaks

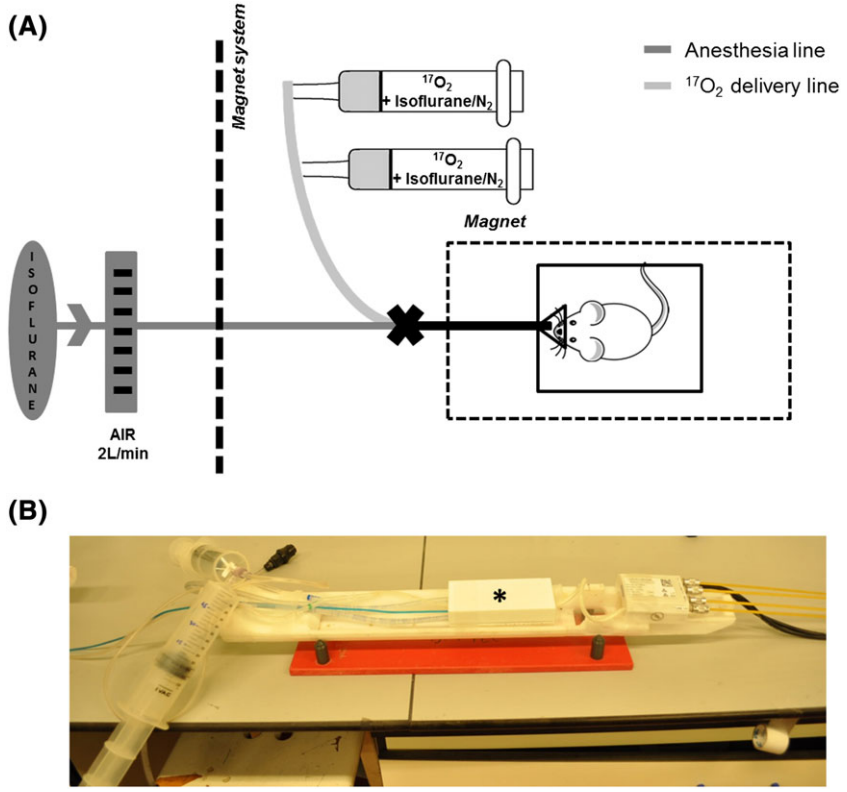

FIGURE 1 Gas delivery system. A, illustration of the breathing system used to deliver $^{17}O_2$. (B) a closed home-built system (*) was used to hold the animal during the experiments. This system contained space for a nose cone, a circulating water system for body temperature regulation, a breathing monitoring system and the radiofrequency (RF) coil

over time were measured using a home-built program written in Matlab (The MathWorks Inc., Natick, MA, USA). The $H_2{}^{17}O$ signal was then expressed relative to the mean baseline signal before $^{17}O_2$ delivery. The mean signal of the final steady state (s_{final}) during the post-inhalation period was calculated between 1100 and 1200 s. We considered that the steady state was reached when the signal stood between $s_{final} \pm 5\%$ of signal variation. For each experiment, the slope during the linear incorporation phase was measured between 600 s and the time point at which steady state was reached.

We randomly separated mice into two distinct cohorts to undergo normothermic or hypothermic conditions. For normothermic conditions, basal measurements were performed. For mild hypothermic conditions, experiments were started 2 h after the mice reached 32°C.

To estimate the signal contribution of both the tumor and muscle compartments during oxygen consumption measurements, a three-dimensional fast low-angle shot (3D FLASH) image of a sample filled with $H_2{}^{17}O$ (0.5%) and H_2O (TR = 12 ms; FA, 20°; matrix, 32 × 32 × 32; FOV, 32 × 32 × 32 mm^3; NA, 4096) was first obtained with the ^{17}O coil to map the signal obtained within the detection area. Second, the tumor area and the surrounding muscle area were delimited on every slice in a set of anatomical images of a typical tumor. With the combined information of the signal from the ^{17}O coil and the region of interest (ROI) from tumor and muscle, the ratio of contribution from both compartments was estimated.

2.5 | Statistical analysis

Analysis was performed using Graphpad software. Results were expressed as the mean value of the parameter ± standard error of the mean (SEM). Paired *t*-test was used to compare mean changes in pO_2 values for each condition (32°C or 37°C), and unpaired *t*-test was used to compare mean changes in the $H_2{}^{17}O$ signal between the two conditions. For all tests, results with $p < 0.05$ (*), $p < 0.01$ (**) or $p < 0.001$ (***) were considered to be significant.

3 | RESULTS

3.1 | Effect of mild hypothermia on tumor oxygenation

Using EPR oximetry, pO_2 levels of FSAII tumors were monitored after the induction of mild hypothermia (32°C), as presented in Figure 2. The basal measured pO_2 (mean ± SEM) was 3.6 ± 0.3 mmHg. The tumors displayed a systematic increase in their oxygenation level 30 min after hypothermia induction. The maximal pO_2 was reached after ~90 min, with a mean pO_2 of 5.9 ± 0.3 mmHg. This value was significantly higher than the baseline ($n = 5$, $p = 0.0005$). No oxygenation changes were observed for mice kept under normothermic (37°C) conditions during 2 h ($n = 4$, $p = 0.1028$ after 2 h).

3.2 | Effect of mild hypothermia on tumor oxygen consumption

In Figure 3, a typical evolution of the $H_2{}^{17}O$ signal is presented for FSAII tumors under normothermic (Figure 3A) and hypothermic (Figure 3B) conditions during ^{17}O MRS experiments. For each condition, the $H_2{}^{17}O$ signal was expressed relative to the mean baseline signal before $^{17}O_2$ delivery. Before $^{17}O_2$ inhalation, the natural abundance $H_2{}^{17}O$ signal was detected. The $H_2{}^{17}O$ signal increased during $^{17}O_2$ inhalation as a result of the inclusion of the ^{17}O atom during metabolism, and reached a new steady state during the

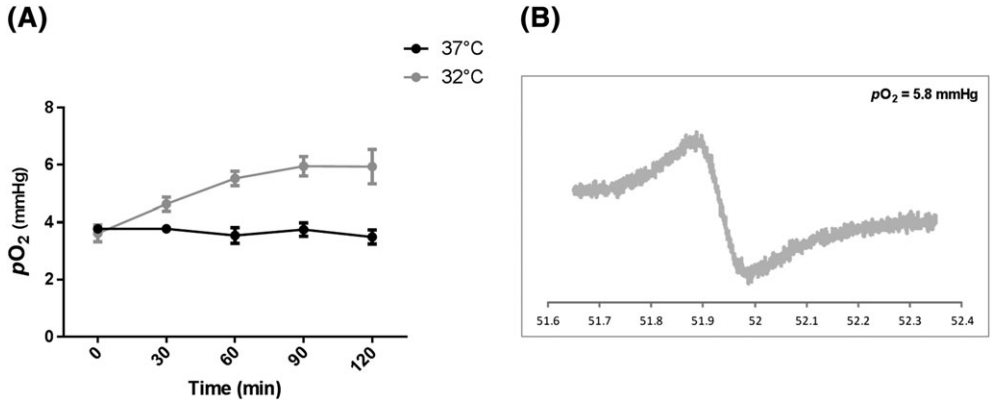

FIGURE 2 Effect of mild hypothermia on tumor oxygenation. A, evolution of pO_2 in tumors under normothermic (37°C) and hypothermic (32°C) conditions, monitored by electron paramagnetic resonance (EPR) oximetry. Data are expressed as means ± standard error of the mean (SEM). (B) typical EPR spectrum recorded *in vivo* under hypothermic conditions

post-inhalation period. Contrary to the observations in previous studies performed in brain[13] and heart[18] tissues, the $H_2{}^{17}O$ signal continued to increase after the oxygen gas was switched to $^{16}O_2$. In addition, we did not observe the exponential decay rate during the post-inhalation phase. These results highlight the impact of the complex tumor vessel architecture and hemodynamics on $^{17}O_2$ metabolism.

Eleven tumors under normothermic conditions and six tumors under hypothermic conditions were scanned. Pooled stacked plots of tumor $H_2{}^{17}O$ spectra are presented in Figure 4. The results were highly reproducible under the same thermic conditions (Figure 4A). In addition, no shift in the resonance frequency was observed during the experiments. For mice kept under mild hypothermia for 2 h, the rate of increase in the $H_2{}^{17}O$ signal was lower compared to animals kept under normothermic conditions ($p = 0.0011$) (Figure 4B). Under hypothermia, FSAII tumors exhibited a slope of $(2.295 \pm 0.26) \times 10^{-4}$ s^{-1}. Under normothermic conditions, the slope was $(6.619 \pm 0.767) \times 10^{-4}$ s^{-1}.

4 | DISCUSSION

In this study, we evaluated the impact of hypothermia on the oxygen consumption rate in tumors using direct ^{17}O MRS. Mild hypothermia

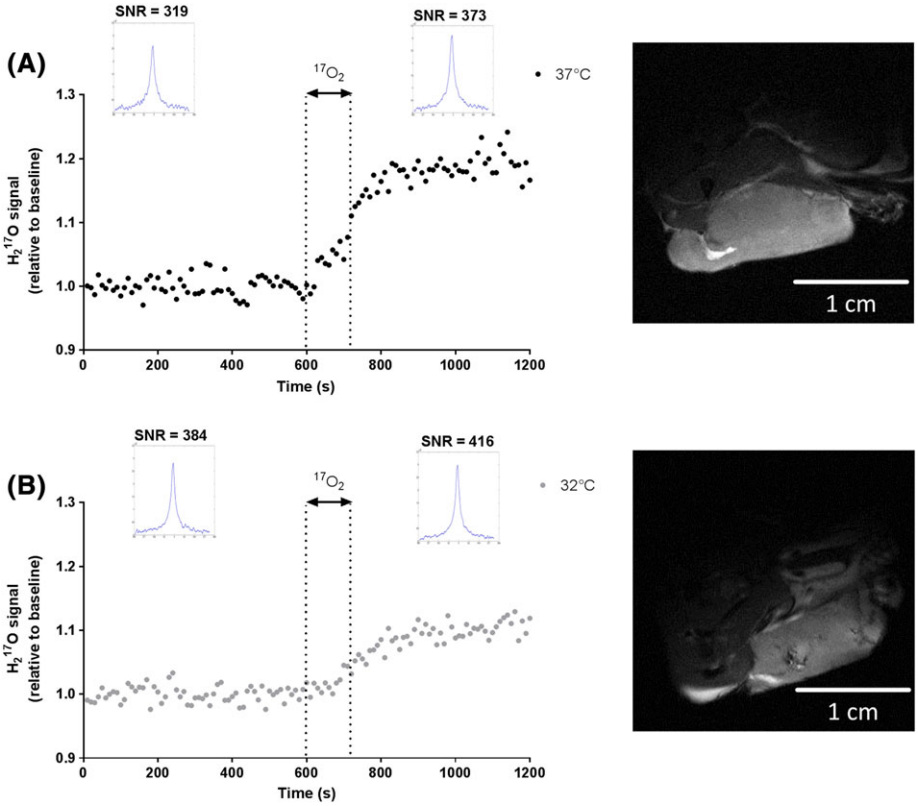

FIGURE 3 $H_2{}^{17}O$ signal from representative tumors under normothermic A, and hypothermic (B) conditions acquired before, during and after a 2-min inhalation period of $^{17}O_2$ gas and corresponding ^1H anatomical images. The $H_2{}^{17}O$ signal is expressed relative to the mean baseline signal before $^{17}O_2$ delivery. The typical $H_2{}^{17}O$ spectra and related signal-to-noise ratio (SNR) for natural abundance (200 s) and final steady state (1000 s) are shown for each condition

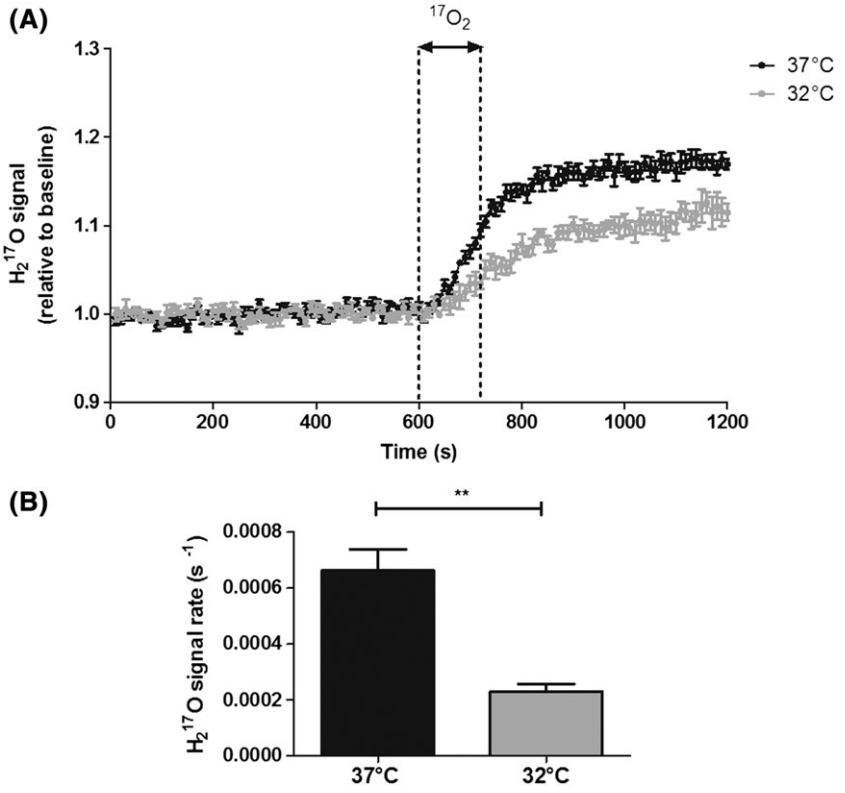

FIGURE 4 Comparison of oxygen consumption in tumors under normothermic (37°C) and hypothermic (32°C) conditions. A, pooled stacked plots of the tumor $H_2{}^{17}O$ signal during $^{17}O_2$ delivery experiments. The $H_2{}^{17}O$ signal is expressed relative to the mean baseline signal before $^{17}O_2$ delivery. (B) comparison of the rate of the $H_2{}^{17}O$ signal after $^{17}O_2$ delivery in tumors. Data are expressed as means ± standard error of the mean (SEM). Unpaired tests were two-sided

is currently used in intensive care units and provides protective effects in traumatic brain injury, cardiopulmonary resuscitation, stroke and various other disorders.[36] Likewise, mild hypothermia has been presented as an attractive tool to modulate oxygen metabolism in tumors. By inducing hypometabolism, the oxygen consumption rate drops, leading to an improvement in tumor oxygenation and a reduction in the hypoxic fraction.[37] Here, we observed an increased in pO_2 values (measured by EPR oximetry) in FSAII tumors 2 h after the induction of mild hypothermia. This increase in tumor oxygenation coincided with a decrease in tumor oxygen consumption (assessed by direct ^{17}O MRS) for mice kept under hypothermic conditions. This suggests that the increase in tumor oxygenation is more likely to result from a decrease in oxygen consumption than a decrease in oxygen delivery induced by hypothermia treatment. These data are consistent with a previous study indicating the effects of hypothermia on the cerebral metabolic rate of oxygen ($CMRO_2$) using direct ^{17}O MRI in rat brain,[38] and validate the ability of direct ^{17}O MRS to assess subtle variations in O_2 consumption rate in tumors.

As the knowledge of cancer metabolism has increased, the ability of cancer cells to remodel biochemical pathways and their amassed metabolic flexibility have become major features of cancer.[39] For a long time, oxygen consumption had been considered to play a minor role in tumor metabolism.[40] However, recent findings have indicated the key role of oxidative pathways in cancer for the maintenance of tumorigenic potential.[23,25,41] Oxygen consumption can also contribute to the hypoxic microenvironment in tumors.[42] Indeed, imbalance between consumption rates and oxygen delivery will result in tumor hypoxia and will affect tumor response to therapies. Likewise, pharmacological modulators of oxygen consumption have been described to improve tumor oxygenation, leading to the enhancement of radiotherapy efficacy.[43-50] Consequently, there is a critical need for sensitive methods to measure the oxygen consumption of tumors non-invasively. Highly sensitive methods have been used to determine cellular oxygen consumption *in vitro*.[51] Several techniques have been described to assess oxygen consumption *in vivo*, such as ^{15}O PET,[52] deuterium NMR,[53,54] ^{19}F MRI,[55,56] blood oxygenation level-dependent (BOLD) MRI,[57] ^{13}C NMR[58] or EPR oximetry.[59] These approaches generally lack specificity, do not provide a direct measurement of O_2 consumption and cannot always provide quantitative information. For some of them, a long measurement time and extensive modeling are required. Nevertheless, they constitute methods of choice for a better assessment of cell bioenergetics, especially in combination with robust approaches, such as ^{17}O MRS/MRI. The potential of following $H_2{}^{17}O$ by ^{17}O MRS/MRI as a tracer for oxygen consumption has been explored using different approaches. The detection of $H_2{}^{17}O$ distribution by indirect ^1H–(^{17}O) methods,[60-63] exploiting the impact of ^{17}O on ^1H relaxation properties, has the advantage to rely on the high sensitivity of the proton signal and can be applied using conventional MRI scanner systems. However, difficulties in the quantitative correlation of ^1H signal changes with $H_2{}^{17}O$ concentration, and the impact of many physiological parameters on the indirect measurements, represent major challenges for the absolute quantification of the $H_2{}^{17}O$ concentration (as reviewed by Zhu and Chen[16]). On the contrary, direct ^{17}O MRS/MRI involves the specific detection of $H_2{}^{17}O$ and can detect small dynamic changes in metabolic $H_2{}^{17}O$, especially at high magnetic field,[12] but requires dedicated RF coils and ultra-fast MR sequences. However, this NMR technique provides a robust, direct, fast and non-invasive way to appraise oxygen consumption *in vivo* and could potentially be applied to numerous tissues.

Recent studies have investigated the use of direct ^{17}O MRI to measure oxygen metabolism in tumors.[19,20] In the study of Narazaki

et al.,[19] the ^{17}O signal was measured by 10 min of data accumulation before and 40 min after a brief inhalation of $^{17}O_2$ gas. These authors identified an increase in the signal intensity in ^{17}O images of tumor-bearing mice after $^{17}O_2$ gas inhalation. Hoffmann et al.[20] recently attempted to determine $CMRO_2$ in a patient with glioblastoma by ^{17}O MRI. Large differences in the signal increase during $^{17}O_2$ inhalation were obtained for white matter, gray matter and different tumor areas of the patient. Although these two studies presented the first attempts to evaluate oxygen consumption in preclinical tumor models and in a patient with glioblastoma, respectively, the present study adds to this in several ways. First, we demonstrated the feasibility of the non-invasive quantification of oxygen consumption in tumors using direct ^{17}O MRS *in vivo*. Quantification models have been developed to determine the oxygen consumption rate in the brain.[14,15] Using an empirical model, we measured the slope during the linear incorporation phase to assess oxygen consumption. This model was able to reflect the oxygen consumption rates in our tumor model and demonstrated adequate reproducibility within groups. Second, we identified that complex vessel architecture and hemodynamics in tumors have a major impact on $^{17}O_2$ metabolism and $H_2{}^{17}O$ signal evolution. Delayed local $H_2{}^{17}O$ production could reflect the delayed arrival of $^{17}O_2$ in the tumor. In addition, a reduced washout could also explain the absence of the exponential decay rate during the post-inhalation phase. These results are consistent with those of Zhu et al.,[64] who evaluated oxygen metabolism and blood perfusion in stroke mice. In this study, they also observed that large reductions in both $CMRO_2$ and cerebral blood flow significantly affected the $H_2{}^{17}O$ signal curve in the brain. Finally, we assessed the value of the method to highlight differences in the oxygen consumption rate in tumors. As the technique was able to reveal the effect of a modulator of tumor oxygenation (hypothermia treatment), direct ^{17}O MRS could represent a relevant tool for tumor metabolic profiling *in vivo* and could potentially be translated to human patients to guide treatments targeting tumor metabolism.

However, our study presents some limitations that should be addressed. First, the slope of the $H_2{}^{17}O$ signal during $^{17}O_2$ inhalation was used to determine oxygen metabolism in the tumor. This empirical method was inspired by models originally established to assess $CMRO_2$ in rodent brain. However, the measured $H_2{}^{17}O$ signal during $^{17}O_2$ delivery is a result of both the local generation of $H_2{}^{17}O$ (produced during local $^{17}O_2$ consumption) and blood recirculation of $H_2{}^{17}O$ (generated throughout the body). As the blood flow was not determined in the current study, this could lead to an overestimation of the oxygen consumption rate in the tissue. Complete models previously reported in the literature for $CMRO_2$ quantification should be considered.[14,15] Nevertheless, their relevance in tumors should first be established. The complex tumor vasculature could limit the applicability of these models to assess oxygen consumption in tumors. Second, because of the large volume covered by the $^{1}H/^{17}O$ coil and the use of a non-localized sequence for the ^{17}O MRS experiments, we cannot exclude the contamination coming from surrounding tissues also affected by hypothermia. We estimated a higher signal contribution from the tumor, but significant impact of the environment has also been observed (signal ratio of 57% *versus* 43% from tumor and surrounding tissue, respectively). To evaluate the impact of surrounding muscle during our measurements, we also assessed the impact of mild hypothermia in the contralateral leg of tumor-bearing mice. $^{17}O_2$ metabolism in muscle was slightly affected by hypothermia treatment. The oxygen consumption rate was only decreased by 7% under hypothermic relative to normothermic conditions (Supporting Information Figure S1). As a drop of 65% of the oxygen consumption rate was assessed in tumors, we can assume a limited impact of surrounding muscle during our measurements. Nevertheless, localized methods and the application of parametric maps should be preferred to avoid interference with surrounding tissues and to reveal the metabolic heterogeneity in tumors.

In conclusion, our study reveals the emergence of a new field of application for direct ^{17}O MRS in oncology. The technique reveals subtle variations in the O_2 consumption rate in tumors induced by hypothermic treatment. Therefore, the technique provides a unique way to study non-invasively *in vivo* an important aspect of tumor metabolism and could have a significant impact in oncology research.

ACKNOWLEDGEMENTS

This study was supported by grants from the Belgian National Fund for Scientific Research (FNRS) - Grant PDR T.0107.13, the Televie (7.4578.13) and the Action de Recherches Concertées 14/19-058. M.-A.N. and B.F.J. are a research fellow and a senior research associate, respectively, of the FNRS. The authors would like to thank Drs Xiao-Hong Zhu and Michiko Narazaki for helpful discussions.

REFERENCES

1. Civan MM, Shporer M. Pulsed nuclear magnetic resonance study of (17)O, (2)D, and (1)H of water in frog striated muscle. *Biophys J*. 1975;15(4):299-306.
2. Shporer M, Haas M, Civan MM. Pulsed nuclear magnetic resonance study of (17)O from H(2)(17)O in rat lymphocytes. *Biophys J*. 1976;16(6):601-611.
3. Fung BM, McGaughy YW. Study of spin-lattice and spin-spin relaxation times of (1)H, (2)H and (17)O in muscular water. *Biophys J*. 1979;28(2):293-303.
4. Mateescu GD, Yvars GM, Dular T. Oxygen-17 magnetic resonance imaging. *Proceedings of the 6th Annual Meeting ISMRM*, New York, USA, 1987; 929.
5. Mateescu GD, Yvars GM, Pazara DI, et al. Combined $^{17}O/^{1}H$ magnetic resonance microscopy in plants, animals and materials: present status and potential. In: Baillie TA, Jones JR, eds. *Synthesis and Applications of Isotopically Labelled Compounds*. Amsterdam: Elsevier Science Publishers; 1988:499-508.
6. Mateescu GD, Yvars GM, Dular T. Water, ions and O-17 magnetic resonance imaging. In: Läuger P, Packer L, Vasilescu V, eds. *Water and Ions in Biological Systems*. Basel, Boston, Berlin: Birkhäuser Verlag; 1988:239-250.
7. Mateescu GD, Yvars GM, LaManna JC, Lust WD, Sudilowski D. In vivo evaluation of water uptake and residence time in the mouse brain after injection of O-17 labelled water. *Proceedings of the 9th Annual Meeting ISMRM*, New York, USA, 1990; 1236.
8. Arai T, Nakao S, Mori K, et al. Cerebral oxygen utilization analyzed by the use of oxygen-17 and its nuclear magnetic resonance. *Biochem Biophys Res Commun*. 1990;169(1):153-158.
9. Mateescu GD, LaManna JC, Lust WD, Mars L, Tseng J. Oxygen-17 magnetic resonance: In vivo determination of nascent mitochondrial water in animals breathing ^{17}O-enriched air. *Proceedings of the 10th Annual Meeting ISMRM*, San Francisco, CA, USA, 1991;1031.

10. Pekar J, Ligeti L, Ruttner Z, et al. In vivo measurement of cerebral oxygen consumption and blood flow using ^{17}O magnetic resonance imaging. *Magn Reson Med*. 1991;179(2):954-961.
11. Arai T, Mori K, Nakao S, et al. In vivo oxygen-17 nuclear magnetic resonance for the estimation of cerebral blood flow and oxygen consumption. *Biochem Biophys Res Commun*. 1991;179(2):954-961.
12. Zhu XH, Merkle H, Kwag JH, Ugurbil K, Chen W. ^{17}O relaxation time and NMR sensitivity of cerebral water and their field dependence. *Magn Reson Med*. 2001;45(4):543-549.
13. Zhu XH, Zhang Y, Tian RX, et al. Development of (17)O NMR approach for fast imaging of cerebral metabolic rate of oxygen in rat brain at high field. *Proc Natl Acad Sci U S A*. 2002;99(20):13194-13199.
14. Zhu XH, Zhang N, Zhang Y, Zhang X, Ugurbil K, Chen W. In vivo ^{17}O NMR approaches for brain study at high field. *NMR Biomed*. 2005;18(2):83-103.
15. Atkinson IC, Thulborn KR. Feasibility of mapping the tissue mass corrected bioscale of cerebral metabolic rate of oxygen consumption using 17-oxygen and 23-sodium MR imaging in a human brain at 9.4 T. *Neuroimage*. 2010;51(2):723-733.
16. Zhu XH, Chen W. In vivo oxygen-17 NMR for imaging brain oxygen metabolism at high field. *Prog Nucl Magn Reson Spectrosc*. 2011;59(4):319-335.
17. Lu M, Atthe B, Mateescu GD, Flask CA, Yu X. Assessing mitochondrial respiration in isolated hearts using (17)O MRS. *NMR Biomed*. 2012;25(6):883-889.
18. Zhu XH, Zhang Y, Chen W. In vivo ^{17}O MRS imaging for assessing myocardial oxygen metabolism in rat heart at 9.4 T. *Proceedings of the 18th Annual Meeting ISMRM*, Stockholm, Sweden, 2010;172.
19. Narazaki M, Kanazawa Y, Koike S, Ando K, Ikehira H. Quantitative ^{17}O imaging towards oxygen consumption study in tumor bearing mice at 7 T. *Magn Reson Imaging*. 2013;31(5):643-650.
20. Hoffmann SH, Radbruch A, Bock M, Semmler W, Nagel AM. Direct (17) O MRI with partial volume correction: First experiences in a glioblastoma patient. *MAGMA*. 2014;27(6):579-587.
21. Warburg O. Uber den Stoffwechsel der Carcinomzelle. *Klin Wochenschr*. 1925;4:534-536.
22. Gatenby RA, Gillies RJ. Why do cancers have high aerobic glycolysis? *Nat Rev Cancer*. 2004;4(11):891-899.
23. Moreno-Sanchez R, Rodriguez-Enriquez S, Marin-Hernandez A, Saavedra E. Energy metabolism in tumor cells. *FEBS J*. 2007;274(6):1393-1418.
24. Jose C, Bellance N, Rossignol R. Choosing between glycolysis and oxidative phosphorylation: A tumor's dilemma? *Biochim Biophys Acta*. 2011;1807(6):552-561.
25. Viale A, Corti D, Draetta GF. Tumors and mitochondrial respiration: A neglected connection. *Cancer Res*. 2015;75(18):3685-3686.
26. Mateescu GD, Cabrera ME. In vivo O-17 magnetic resonance spectroscopy. Determination of temperature effects on metabolic rates (Q10 factor). *Adv Exp Med Biol*. 1997;411:585-590.
27. Ansiaux R, Baudelet C, Jordan BF, et al. Thalidomide radiosensitizes tumors through early changes in the tumor microenvironment. *Clin Cancer Res*. 2005;11(2 Pt 1):743-750.
28. Karroum O, Mignion L, Kengen J, et al. Multimodal imaging of tumor response to sorafenib combined with radiation therapy: Comparison between diffusion-weighted MRI, choline spectroscopy and ^{18}F-FLT PET imaging. *CMMI*. 2013;8(3):274-280.
29. Baudelet C, Gallez B. Effect of anesthesia on the signal intensity in tumors using BOLD-MRI: Comparison with flow measurements by laser Doppler flowmetry and oxygen measurements by luminescence-based probes. *Magn Reson Imaging*. 2004;22(7):905-912.
30. Tran LB, Bol A, Labar D, et al. Hypoxia imaging with the nitroimidazole ^{18}F-FAZA PET tracer: A comparison with OxyLite, EPR oximetry and ^{19}F-MRI relaxometry. *Radiother Oncol*. 2012;105(1):29-35.
31. Colliez F, Neveu MA, Magat J, Cao Pham TT, Gallez B, Jordan BF. Qualification of a noninvasive magnetic resonance imaging biomarker to assess tumor oxygenation. *Clin Cancer Res*. 2014;20(21):5403–5411.
32. Danhier P, Gallez B. Electron paramagnetic resonance: A powerful tool to support magnetic resonance imaging research. *CMMI*. 2015;10(4):266-281.
33. Gallez B, Jordan BF, Baudelet C, Misson PD. Pharmacological modifications of the partial pressure of oxygen in murine tumors: Evaluation using in vivo EPR oximetry. *Magn Reson Med*. 1999;42(4):627-630.
34. Jordan BF, Baudelet C, Gallez B. Carbon-centered radicals as oxygen sensors for in vivo electron paramagnetic resonance: Screening for an optimal probe among commercially available charcoals. *MAGMA*. 1998;7(2):121-129.
35. Gallez B, Baudelet C, Jordan BF. Assessment of tumor oxygenation by electron paramagnetic resonance: Principles and applications. *NMR Biomed*. 2004;17(5):240-262.
36. Polderman KH. Application of therapeutic hypothermia in the ICU: Opportunities and pitfalls of a promising treatment modality. Part 1: Indications and evidence. *Intensive Care Med*. 2004;30(4):556-575.
37. Kelleher DK, Nauth C, Thews O, Krueger W, Vaupel P. Localized hypothermia: Impact on oxygenation, microregional perfusion, metabolic and bioenergetic status of subcutaneous rat tumours. *Br J Cancer*. 1998;78(1):56-61.
38. Zhu XH, Zhang Y, Zhang N, Ugurbil K, Chen W. Noninvasive and three-dimensional imaging of CMRO(2) in rats at 9.4 T: Reproducibility test and normothermia/hypothermia comparison study. *J Cereb Blood Flow Metab*. 2007;27(6):1225-1234.
39. Hanahan D, Weinberg RA. Hallmarks of cancer: The next generation. *Cell*. 2011;144(5):646-674.
40. Warburg O. On respiratory impairment in cancer cells. *Science*. 1956;124(3215):269-270.
41. Moreno-Sanchez R, Marin-Hernandez A, Saavedra E, Pardo JP, Ralph SJ, Rodriguez-Enriquez S. Who controls the ATP supply in cancer cells? Biochemistry lessons to understand cancer energy metabolism. *Int J Biochem Cell Biol*. 2014;50:10-23.
42. Höckel M, Vaupel P. Tumor hypoxia: Definitions and current clinical, biologic, and molecular aspects. *J Natl Cancer Inst*. 2001;93(4):266-276.
43. Jordan BF, Grégoire V, Demeure RJ, et al. Insulin increases the sensitivity of tumors to irradiation: Involvement of an increase in tumor oxygenation mediated by a nitric oxide-dependent decrease of the tumor cells oxygen consumption. *Cancer Res*. 2002;62(12):3555-3561.
44. Crokart N, Radermacher K, Jordan BF, et al. Tumor radiosensitization by antiinflammatory drugs: Evidence for a new mechanism involving the oxygen effect. *Cancer Res*. 2005;65(17):7911-7916.
45. Crokart N, Jordan BF, Baudelet C, et al. Glucocorticoids modulate tumor radiation response through a decrease in tumor oxygen consumption. *Clin Cancer Res*. 2007;13(2 Pt 1):630-635.
46. Jordan BF, Sonveaux P, Feron O, et al. Nitric oxide as a radiosensitizer: Evidence for an intrinsic role in addition to its effect on oxygen delivery and consumption. *Int J Cancer*. 2004;109(5):768-773.
47. Jordan BF, Peeterbroeck J, Karroum O, et al. Captopril and S-nitrosocaptopril as potent radiosensitizers: Comparative study and underlying mechanisms. *Cancer Lett*. 2010;293(2):213-219.
48. Diepart C, Karroum O, Magat J, et al. Arsenic trioxide treatment decreases the oxygen consumption rate of tumor cells and radiosensitizes solid tumors. *Cancer Res*. 2012;72(2):482-490.
49. Ansiaux R, Dewever J, Gregoire V, Feron O, Jordan BF, Gallez B. Decrease in tumor cell oxygen consumption after treatment with vandetanib (ZACTIMA; ZD6474) and its effect on response to radiotherapy. *Radiat Res*. 2009;172(5):584-591.
50. Jordan BF, Christian N, Crokart N, Grégoire V, Feron O, Gallez B. Thyroid status is a key modulator of tumor oxygenation: Implication for radiation therapy. *Radiat Res*. 2007;168(4):428-432.

51. Diepart C, Verrax J, Calderon PB, Feron O, Jordan BF, Gallez B. Comparison of methods for measuring oxygen consumption in tumor cells in vitro. *Anal Biochem*. 2010;396(2):250-256.
52. Baron JC, Jones T. Oxygen metabolism, oxygen extraction and positron emission tomography: Historical perspective and impact on basic and clinical neuroscience. *Neuroimage*. 2012;61(2):492-504.
53. Mateescu GD, Ye A, Flask CA, Erowku B, Duerk JL. In vivo assessment of oxygen consumption via deuterium magnetic resonance. *Adv Exp Med Biol*. 2011;701:193-199.
54. Mateescu GD, Flask CA, Ye A, et al. Novel biomarkers of mitochondrial function: The mitochondrial index and the crossing point of glucose and oxygen consumption curves obtained in vivo by dynamic deuterium magnetic resonance. *Proceedings of the 23rd Annual Meeting ISMRM*, Toronto, ON, Canada, 2015; 19.
55. Zhao D, Ran S, Constantinescu A, Hahn EW, Mason RP. Tumor oxygen dynamics: Correlation of in vivo MRI with histological findings. *Neoplasia*. 2003;5(4):308-318.
56. Diepart C, Magat J, Jordan BF, Gallez B. In vivo mapping of tumor oxygen consumption using (19)F MRI relaxometry. *NMR Biomed*. 2011;24(5):458-463.
57. Coquery N, Francois O, Lemasson B, et al. Microvascular MRI and unsupervised clustering yields histology-resembling images in two rat models of glioma. *J Cereb Blood Flow Metab*. 2014;34(8):1354-1362.
58. Shestov AA, Lee SC, Nath K, et al. (13)C MRS and LC-MS flux analysis of tumor intermediary metabolism. *Front. Oncologia*. 2016;6:135.
59. Diepart C, Jordan BF, Gallez B. A new EPR oximetry protocol to estimate the tissue oxygen consumption in vivo. *Radiat Res*. 2009;172(2):220-225.
60. Mellon EA, Beesam RS, Elliott MA, Reddy R. Mapping of cerebral oxidative metabolism with MRI. *Proc Natl Acad Sci U S A*. 2010;107(26):11787-11792.
61. Mellon EA, Beesam RS, Baumgardner JE, Borthakur A, Witschey WR 2nd, Reddy R. Estimation of the regional cerebral metabolic rate of oxygen consumption with proton detected ^{17}O MRI during precision $^{17}O_2$ inhalation in swine. *J Neurosci Methods*. 2009;179(1):29-39.
62. Tailor DR, Baumgardner JE, Regatte RR, Leigh JS, Reddy R. Proton MRI of metabolically produced $H_2{}^{17}O$ using an efficient $^{17}O_2$ delivery system. *Neuroimage*. 2004;22(2):611-618.
63. Hopkins AL, Barr RG. Oxygen-17 compounds as potential NMR T2 contrast agents: Enrichment effects of H2(17)O on protein solutions and living tissues. *Magn Reson Med*. 1987;4(4):399-403.
64. Zhu XH, Chen JM, Tu TW, Chen W, Song SK. Simultaneous and noninvasive imaging of cerebral oxygen metabolic rate, blood flow and oxygen extraction fraction in stroke mice. *Neuroimage*. 2013;64:437-447.

SUPPORTING INFORMATION

Additional Supporting Information may be found online in the supporting information tab for this article.

How to cite this article: Neveu M-A, Joudiou N, De Preter G, Dehoux J-P, Jordan BF, Gallez B. ^{17}O MRS assesses the effect of mild hypothermia on oxygen consumption rate in tumors. *NMR in Biomedicine*. 2017;e3726. https://doi.org/10.1002/nbm.3726